Chemical Science

Accepted Manuscript

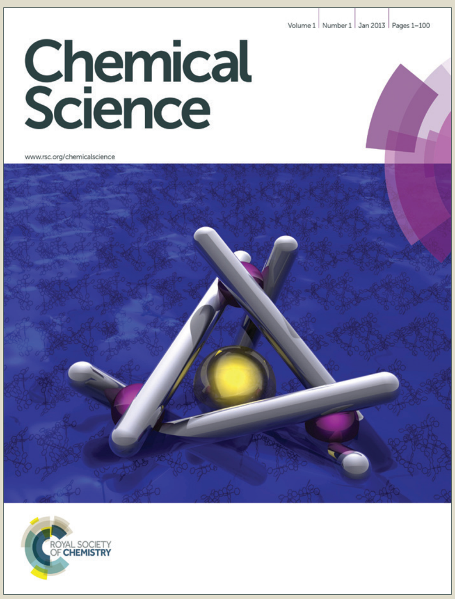

Journal Name

RSCPublishing

ARTICLE

5,20-Bis(α-oligothienyl)-substituted [26]hexaphyrins possessing electronic circuits strongly perturbed by *meso*-oligothienyl substituents

Cite this: DOI: 10.1039/x0xx00000x

Received 00th January 2012,
Accepted 00th January 2012

DOI: 10.1039/x0xx00000x

www.rsc.org/

Hirotaka Mori,[a] Masaaki Suzuki,[a] Woojae Kim,[b] Dongho Kim,*[b] and Atsuhiro Osuka*[a]

A series of [26]hexaphyrins(1.1.1.1.1.1) bearing two α-oligothienyl substituents at 5,20-positions have been synthesised and shown to take a dumbbell hexaphyrin conformation, to which the α-oligothienyl groups are linked with small dihedral angles to form an acyclic helix-like conjugated network. While their distinct diatropic ring currents and reversible four reduction waves characteristic of aromatic [26]hexaphyrins indicate that the [26]hexaphyrin aromatic circuits are viable, the absorption spectra and excited state dynamics are significantly perturbed, which becomes increasingly evident with elongation of the oligothienyl substituents. DFT calculations of these hexaphyrins indicated LUMO and LUMO+1 localised on the hexaphyrin circuit and HOMO and HOMO–1 spread over the acyclic helix-like conjugation network, which can explain the perturbed absorption spectra.

Introduction

In the last two decades, the chemistry of expanded porphyrin has gained increasing popularity in light of flexible structures, multi-metal coordination properties, anion sensing abilities, facile interconversions between multiple and neutral redox states, and unprecedented chemical reactivities such as drastic skeletal rearrangements.[1] Fairly flexible electronic systems of *meso*-aryl expanded porphyrins have been demonstrated by exploration of versatile electronic states such as Hückel aromatic, Hückel antiaromatic,[2] Möbius aromatic,[3] Möbius antiaromatic,[4] stable monoradical,[5] and singlet biradicaloid species.[6] As an additional example, internally 5,20-aromatics-bridged [26]hexaphyrins have been recently developed as a dual electronic system consisting of [18]porphyrin and/or [26]hexaphyrin, which can be modulated by the internal bridging aromatic unit (Figure 1a).[7] In this paper, we report the synthesis of a series of 5,20-bis(α-oligothienyl) [26]hexaphyrins(1.1.1.1.1.1) (**T2**–**T4**), which display characteristic optical and electronic properties due to the presence of 5,20-bis(α-oligothienyl) substituents (Figure 1b).

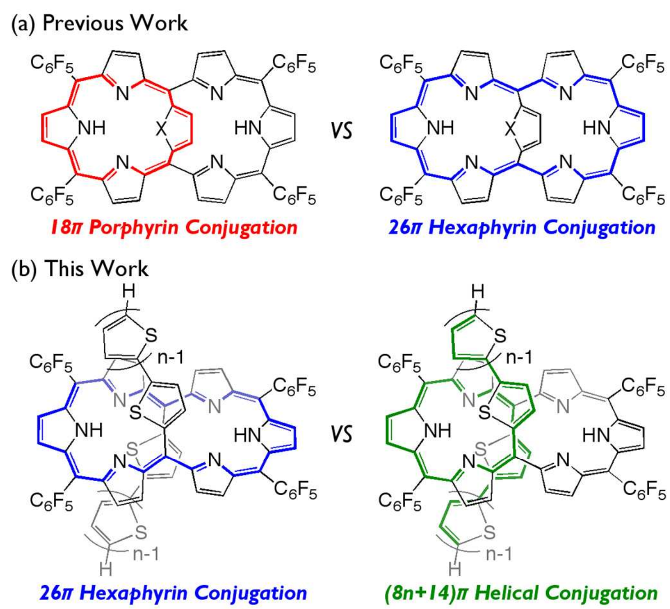

Fig. 1. [26]Hexaphyrins possessing dual electronic systems; a) internally aromatics-bridged [26]hexaphyrins (X = S, NH) and b) bis(α-oligothienyl) [26]hexaphyrins. Effective conjugated networks are indicated by coloured lines.

Results and Discussion

Synthesis of 5,20-bis(α-oligothienyl) [26]hexaphyrins(1.1.1.1.1.1)

[26]Hexaphyrins **T2**–**T4** have been prepared by a modified method used for the synthesis of 5,20-(2-thienyl) [26]hexaphyrin(1.1.1.1.1.1) **T1**.[8] Acid-catalysed condensation of 5,10-bis(pentafluorophenyl)tripyrrane **1** with corresponding α-oligothiophene-5-carbaldehydes followed by oxidation with 2,3-dichloro-5,6-dicyano-1,4-benzoquinone (DDQ) gave **T2**–**T4** in 22, 10, and 15% yields, respectively (Scheme 1). High-resolution electrospray ionisation time-of-flight (HR ESI-TOF) mass measurements showed the parent ion peaks at m/z = 1457.0685 ([M+H]$^+$; calcd for $C_{70}H_{25}N_6F_{20}S_4$: 1457.0699) for **T2**, m/z 1621.0462 ([M+H]$^+$; calcd for $C_{78}H_{29}N_6F_{20}S_6$: 1621.0453) for **T3**, and m/z 1783.0059 ([M–H]$^-$; calcd for $C_{86}H_{31}N_6F_{20}S_8$: 1783.0062) for **T4** (See Electronic Supplementary Information; ESI). 5,15-Bis(α-oligothienyl)-substituted porphyrins **P1**–**P4** were also prepared (SI) to examine the effects of α-oligothienyl substituents on the electronic system of porphyrins, which highlights the characteristically flexible electronic properties of [26]hexaphyrins.

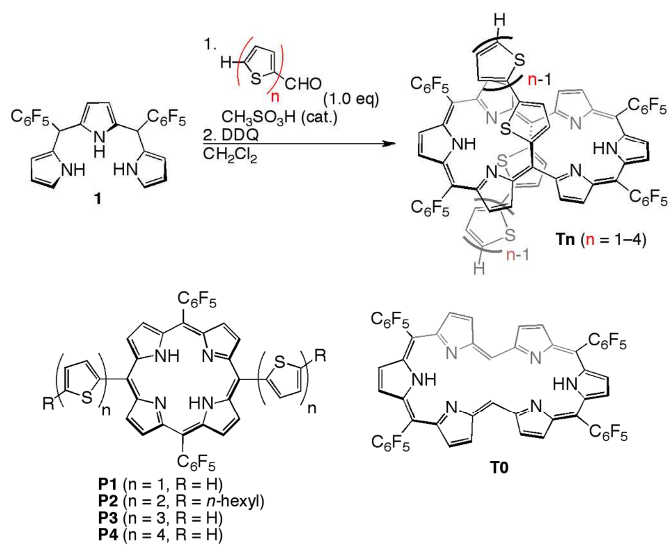

Scheme 1. Synthesis of 5,20-(α-oligothienyl)-substituted [26]hexaphyrins **T1–T4** and structures of **P1–P4**.

The solid-state structures of **T2**–**T4** have been unambiguously determined by single crystal X-ray diffraction analysis.[9] Hexaphyrins **T2**–**T4** all show a dumbbell hexaphyrin conformation, to which the two oligothienyl groups are appended with small dihedral angles, being favorable for conjugation with the hexaphyrin macrocycle (Figure 2 and SI). The hexaphyrin frames of **T2**–**T4** are essentially the same as those of 5,20-unsubstituted hexaphyrin (**T0**)[5a] and **T1**[8] with regard to planar dumbbell structure. Dumbbell conformation is intrinsically the most stable for [26]hexaphyrins, because of energy-stabilising four possible intramolecular hydrogen bonding interactions but is only allowed for [26]hexaphyrins bearing small substituents at 5,20-positions.[5a,8] Thus, **T0** is the most stable, taking a strain-free fairly planar conformation with the largest diatropic ring current. The observed dumbbell structures of **T1**–**T4** have been similarly ascribed to small 2-thienyl and α-oligothienyl substituents.[8] The two oligothienyl substituents are positioned above and below the macrocycle and are orienting toward the same side of the hexaphyrin to form a helix-like conjugated network involving the tripyrrodimethene segments of the hexaphyrin.

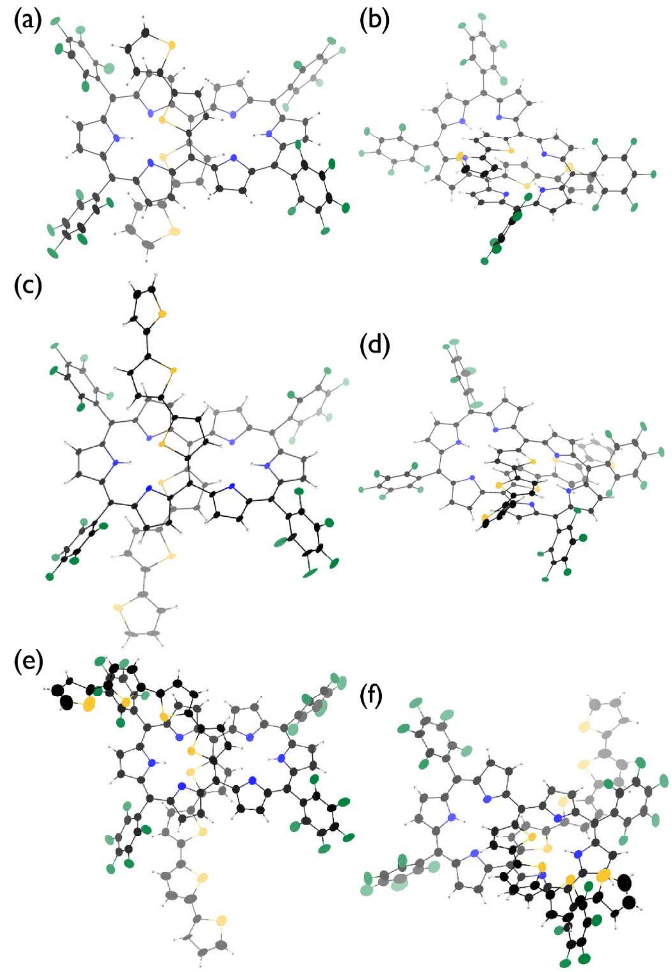

Fig. 2. X-Ray crystal structures of (a,b) **T2**, (c,d) **T3**, and (e,f) **T4**. Solvent molecules are omitted for clarity. The thermal ellipsoids are scaled to 30% probability level. One of the two molecules in the unit cell is shown for **T2** and **T4**.

The ^{1}H NMR spectra of **T0** and **T1** indicate sharp signals at room temperature, which are consistent with the dumbbell structures.[5a,8] The ^{1}H NMR spectrum of **T1** exhibits only three signals at 7.38, 7.72, and 8.16 ppm due to the outer β-pyrrolic protons, indicating a very rapid rotation of the *meso*-thienyl substituents. In contrast, the ^{1}H NMR spectra of **T2**–**T4** taken at room temperature are interesting, in that the protons of the hexaphyrin periphery appear as very broad signals but the protons of the oligothienyl substituents appear as sharp signals. At –60 °C, these ^{1}H NMR spectra became sharp, featuring six signals due to the outer β- pyrrolic protons in the range δ = 8.21 –5.76 ppm and signals due to the *meso*-oligothienyl groups in the range δ = 7.25–4.06 ppm. These data indicate substantial diatropic ring currents for the hexaphyrin in **T2**–**T4** in accordance with the solid-state dumbbell structures. Importantly, two singlets due to the two inner NH protons appeared differently around δ = 8.4–8.2 and 5.4–5.1 ppm, implying that the right and left tripyrrodimethene segments of the hexaphyrin are electronically different, owing to the influence of the *meso*-oligothienyl substituents. Most probably the rotational dynamics of the *meso*-oligothienyl substituents are slow at room temperature as compared with ^{1}H NMR time scale.

Redox potentials and UV/Vis/NIR absorption spectra

The electrochemical properties of **T1**–**T4** were examined by cyclic voltammetry (CV) in CH_2Cl_2 containing 0.1 M Bu_4NPF_6 as a supporting electrolyte versus ferrocene/ferrocenium cation (see Figure S20 and Table S1). All the cyclic voltammograms of **T1**–**T4** showed four reversible reduction waves almost at the same potentials, that correspond to stepwise reductions reaching to their 30π states, hence indicating that the 26π hexaphyrin electronic circuits are all viable. On the other hand, the first oxidation potentials appeared at 0.38 V for **T1**, 0.27 V for **T2**, 0.22 V for **T3**, and 0.17 V for **T4**, indicating the rising of the HOMO levels upon elongation of *meso*-oligothienyl chains.

The absorption spectrum of **T0** displays a sharp and intense Soret-like band at 549 nm and weak but distinct Q-bands in the range of 700–1100 nm as a characteristic feature of typical aromatic porphyrinoids. The absorption spectrum of **T1** exhibits an ill-defined Soret-like band at 616 nm and broad Q-bands in the range of 700–1150 nm, which is significantly different from that of **T0**, indicating that the 2-thienyl substituents cause significant perturbation on the electronic state of the [26]hexaphyrin. This trend is increasingly evident upon elongation of oligothienyl chains. Namely, a Soret-like band, characteristic attribute of aromatic [26]hexaphyrins, almost disappears in the absorption spectra of **T2**–**T4**, and instead a broad high-energy band is observed around 350 nm for **T1**, which is red-shifted and intensified with elongation of *meso*-oligothienyl chains.[10] In addition, **T2**–**T4** show broad Q-bands in NIR region. Collectively, these absorption features of **T2**–**T4** are radically different from those of aromatic porphyrinoids, but are rather similar to those of reported acyclic oligopyrromethenes.[11] The absorption spectra of **T1**-**T4** became sharpened upon lowering temperature (SI), indicating the importance of the dynamic motion of the oligothienyl substituents for broadening of the absorption spectra. In sharp contrast, no such drastic changes were observed in the absorption spectra of porphyrin counterparts **P1**–**P4** (Figure 3b), underlining the unique and flexible electronic properties of [26]hexaphyrins.

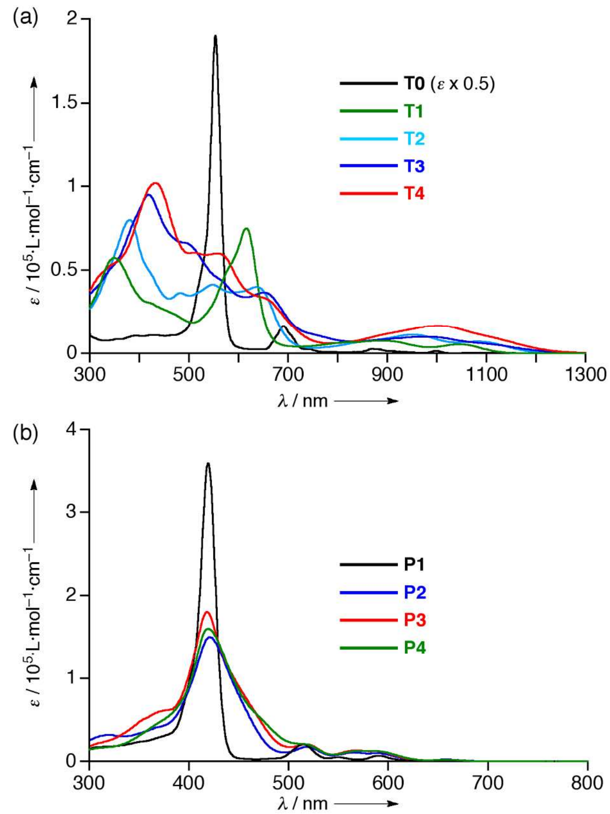

Fig. 3. UV/Vis/NIR absorption spectra of a) **T0–T4** and b) **P1–P4** in CH_2Cl_2.

Theoretical calculations and excited state dynamics

To understand the anomalous absorption spectra, density functional theory (DFT) calculations of **T0**–**T4** were carried out using the Gaussian 09 program at B3LYP/6-31G(d) level.[12] Geometry optimisations produced dumbbell structures that were respectively similar to those obtained via X-ray diffraction analysis. Since calculated MO diagrams of **T2**–**T4** are quite similar (SI), we discuss here MOs of **T3** in comparison with those of **T0**. Similarly to the rectangular shape [26]hexaphyrin,[13] the HOMO and LUMO of **T0** are, respectively, similar to a_{1u} and a_{2u} HOMOs and two degenerate e_g* LUMOs of porphyrins with a HOMO-LUMO gap of 1.88 eV. The LUMO and LUMO+1 of **T3** are nearly localised on the hexaphyrin circuit, and their energy levels are only slightly destabilised from those of **T0**. In contrast, the HOMO–1 is spread over the helix-like network and the HOMO is mainly spread over the same network, and both are largely destabilised, to cause a small HOMO-LUMO gap of 1.340 eV. The MO features of **T2** and **T4** are nearly the same as those of **T3**, which are all consistent with the results of CV. These MO features made us to consider a dual contribution of a 26π-hexaphyrin network and an acyclic conjugation along the helix-like structure (Figure 1b), which plays an important role in the electronic excitation to excited states.

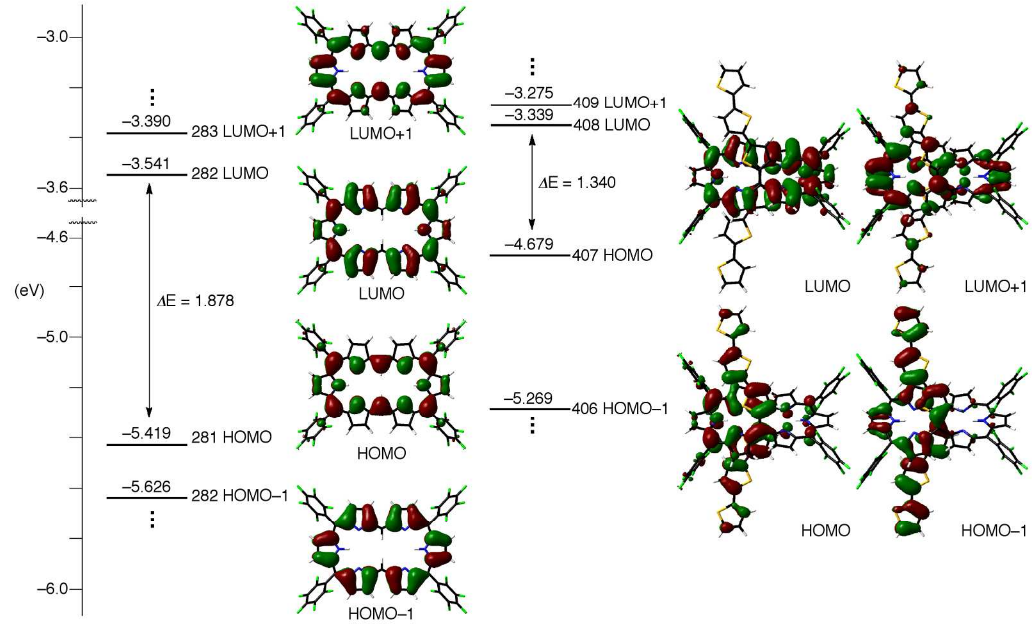

Fig. 4. Kohn-Sham MO diagrams of **T0** and **T3** calculated with Gaussian 09 package. All energy levels were calculated at the B3LYP/6-31G(d) level.

The nucleus-independent chemical shift (NICS) values[14] inside the [26]hexaphyrin macrocycle were calculated to be –15.54, –12.21, –8.50, –8.30, and –8.26 for **T0**–**T4**, respectively. The harmonic oscillator model of aromaticity (HOMA) values[15] for the [26]hexaphyrin circuit were calculated from the real crystal structures and the optimised structures to be 0.783 and 0.737 for **T0**, 0.568 and 0.604 for **T1**, 0.464 (0.425) and 0.518 for **T2**, and 0.397 and 0.498 for **T3**. The HOMA value of **T4** was only calculated for the optimised structure to be 0.498 due to its insufficient crystal data to discuss the bond length. These results indicate the increasing perturbation of the 5,20-oligothienyl substituents from **T1** to **T4**.

We have also investigated the excited state dynamics of **T1**–**T4** by using femtosecond transient absorption (fs-TA) spectroscopy (Figure S46-47) to confirm the electronic perturbation by 5,20-oligothienyl substituents. S1-State lifetimes have been determined to be 35.4 ps for **T1**, 15.2 ps for **T2**, 10.0 ps for **T3**, and 8.5 ps for **T4**, respectively, which shows dramatic decrease as compared to 138 ps for **T0**.[5a] These overall observations also confirmed the increasing electronic perturbation by oligothienyl chains.

Collectively, these experimental and theoretical calculations indicate that the perturbation provided by the oligothienyl substituents is delicate, being not so strong to spoil the aromatic [26]hexaphyrin network but large enough to alter the absorption properties and mitigate the aromatic characters of the [26]hexaphyrin segments as a rare case.

Conclusions

5,20-Bis(α-oligothienyl)-substituted [26]hexaphyrins (1.1.1.1.1.1) **T1**–**T4** were prepared and shown to possess characteristic optical and electronic properties. The observed diatropic ring currents and reversible reduction waves indicate that the aromatic [26]hexaphyrin networks are viable in **T1**–**T4**. Nevertheless, the absorption spectra and the excited state dynamics of **T1**–**T4** are significantly perturbed by the appended oligothienyl substituents. DFT calculations indicated that the LUMO and LUMO+1 are localised at the [26]hexaphyrin network but HOMO and HOMO–1 are significantly spread over the helix-like network and are largely destabilised. Further explorations of expanded porphyrins possessing dual electronic networks are actively underway in our group.

Acknowledgements

The work at Kyoto was supported by JSPS KAKENHI of Grant Numbers 25220802 and 25620031. H.M. acknowledges a JSPS Fellowship for Young Scientists. The work at Yonsei was supported by Global Research Laboratory (GRL) Program (2013-8-1472) of the Ministry of Education, Science, and Technology (MEST) of Korea.

Notes and references

[a]Department of Chemistry, Graduate School of Science, Kyoto University Sakyo-ku, Kyoto 606-8502 (Japan) E-mail: osuka@kuchem.kyoto-u.ac.jp
[b]Spectroscopy Laboratory for Functional π-Electronic Systems and Department of Chemistry Yonsei University, Seoul 120-749 (Korea) E-mail: dongho@yonsei.ac.kr

† Electronic Supplementary Information (ESI) available: [General experimental methods, HR-ESI-TOF mass spectra, UV/vis absorption spectra, NMR spectra, cyclic voltammograms, X-ray crystal structures and results of DFT calculations]. See DOI: 10.1039/b000000x/

1 (a) A. Jasat and D. Dolphin, *Chem. Rev.* 1997, **97**, 2267; (b) H. Furuta, H. Maed and A. Osuka, *Chem. Commun.* 2002, 1795; (c) J. L. Sessler and D. Seidel, *Angew. Chem., Int. Ed.* 2003, **42**, 5134; (d) T. K. Chandrashekar and S. Venkatraman, *Acc. Chem. Res.* 2003, **36**, 676; (e) M. Stępień, N. Sprutta and L. Latos-Grażyński, *Angew. Chem., Int. Ed.* 2011, **50**, 4288; (f) S. Saito,and A. Osuka, *Angew. Chem., Int. Ed.* 2011, **50**, 4342; (g) A. Osuka and S. Saito, *Chem. Commun.* 2011, **47**, 4330.

2 (a) S. Mori and A. Osuka, *J. Am. Chem. Soc.* 2005, **127**, 8030; (b) S. Mori, K. S. Kim, Z. S. Yoon, S. B. Noh, D. Kim and A. Osuka, *J. Am. Chem. Soc.* 2007, **129**, 11344; (c) K. Naoda, H. Mori and A. Osuka, *Chem. Asian J.* 2013, **8**, 1395; (d) H. Mori, Y. M. Sung, B. S. Lee, D. Kim and A. Osuka, *Angew. Chem., Int. Ed.* 2012, **51**, 12459.

3 (a) M. Stępień, L. Latos-Grażyński, N. Sprutta, P. Chwalisz and L. Szterenberg, *Angew. Chem., Int. Ed.* 2007, **46**, 7869; (b) Y. Tanaka, S. Saito, S. Mori, N. Aratani, H. Shinokubo, N. Shibata, Y. Higuchi, Z. S. Yoon, K. S. Kim, S. B. Noh, J. K. Park, D. Kim and A. Osuka, *Angew. Chem., Int. Ed.* 2008, **47**, 681; (c) J. Sankar, S. Mori, S. Saito, H. Rath, M. Suzuki, Y. Inokuma, H. Shinokubo, K. S. Kim, Z. S. Yoon, J.-Y. Shin, J. M. Lim, Y. Matsuzaki, O. Matsushita, A. Muranaka, N. Kobayashi, D. Kim and A. Osuka, *J. Am. Chem. Soc.* 2008, **130**, 13568; (d) Z. S. Yoon, A. Osuka and D. Kim, *Nature Chem.* 2009, **1**, 113.

4 (a) E. Pacholska-Dudziak, J. Skonieczny, M. Pawlicki, L. Szterenberg, Z. Ciunik and L. Latos-Grażyński, *J. Am. Chem. Soc.* 2008, **130**, 6182; (b) T. Higashino, J. M. Lim, T. Miura, S. Saito, J.-Y. Shin, D. Kim and A. Osuka, *Angew. Chem., Int. Ed.* 2010, **49**, 4950; (c) T. Higashino, B. S. Lee, J. M. Lim, D. Kim and A. Osuka, *Angew. Chem., Int. Ed.* 2012, **51**, 13105.

5 (a) T. Koide, G. Kashiwazaki, M. Suzuki, K. Furukawa, M.-C. Yoon, S. Cho, D. Kim and A. Osuka, *Angew. Chem., Int. Ed.* 2008, **47**, 9661; (b) H. Rath, S. Tokuji, N. Aratani, K. Furukawa, J. M. Lim, D. Kim, H. Shinokubo and A. Osuka, *Angew. Chem., Int. Ed.* 2010, **49**, 1489.

6 T. Koide, K. Furukawa, H. Shinokubo, J.-Y. Shin, K. S. Kim, D. Kim and A. Osuka, *J. Am. Chem. Soc.* 2010, **132**, 7246.

7 (a) H. Mori, J. M. Lim, D. Kim and A. Osuka, *Angew. Chem., Int. Ed.* 2013, **52**, 12997; (b) G. Karthik, M. Sneha, V. P. Raja, J. M. Lim, D. Kim, A. Srinivasan and T. K. Chandrashekar, *Chem. Eur. J.* 2013, **19**, 1886.

8 M. Suzuki and A. Osuka, *Chem. Eur. J.* 2007, **13**, 196.

9 (a) Crystallographic data for **T2**: $2(C_{70}H_{24}F_{20}N_6S_4)\cdot 1.82(C_6H_{14})\cdot 1.10(CH_2Cl_2)$, M_r = 3165.36, triclinic, space group *P*-1 (No. 2), a = 18.9073(16), b = 20.7452(6), c = 21.091(2) Å, α = 67.38(2), β = 77.21(2), γ = 65.257(13)°, V = 6917.2(9) Å^3, T = 93 K, ρ_{calcd} = 1.520 g·cm^{-3}, Z = 2, 87882 reflections measured, 23494 unique (R_{int} = 0.0351), R_1 = 0.0639 ($I > 2\sigma(I)$), R_w = 0.1805 (all data), GOF = 1.042; (b) Crystallographic data for **T3**: $C_{78}H_{28}F_{20}N_6S_6\cdot 0.51(C_7H_{16})\cdot C_7\cdot 1.89(CH_2Cl_2)$, *M*r = 1882.68, monoclinic, space group *C*2/*c* (No. 15), a = 49.998(16), b = 12.402(3), c = 35.242(11) Å, β = 131.613(5)°, V = 16338(8) Å^3, T = 93 K, ρ_{calcd} = 1.513 g·cm^{-3}, Z = 8, 51126 reflections measured, 14608 unique (R_{int} = 0.0547), R_1 = 0.0850 ($I > 2\sigma(I)$), R_w = 0.2299 (all data), GOF = 1.034; (c) Crystallographic data for **T4**: $2(C_{86}H_{32}F_{20}N_6S_8)\cdot 2(C_7H_{16})\cdot 0.44(C_7)\cdot 1.53(CHCl_3)\cdot O$, M_r = 4006.31, triclinic, space group *P*-1 (No. 2), a = 17.2734(8), b = 18.9028(5), c = 30.1289(17) Å, α = 105.000(14), β = 92.92(2), γ = 107.23(3)°, V = 8988.7(7) Å^3, T = 93 K, ρ_{calcd} = 1.481 g·cm^{-3}, Z = 2, 99137 reflections measured, 27782 unique (R_{int} = 0.0733), R_1 = 0.1104 ($I > 2\sigma(I)$), R_w = 0.3750 (all data), GOF = 1.073. CCDC 1025770 (for **T2**), 1025771 (for **T3**), and 1025772 (for **T4**) contains the supplementary crystallographic data for this paper. These data can be obtained free of charge from the Cambridge Crystallographic Data Centre via www.ccdc.cam.ac.uk/data_request/cif

10 The intense bands of **T1**–**T4** in UV region are red-shifted in a manner similar to those of α-oligothiophenes as below; 353/354 nm for **T1** and terthiophene, 385/392 nm for **T2** and quaterthiophene, 414/417 nm for **T3** and quinquethiophene, and 432/436 nm for **T4** and sexithiophene. R. S. Becker, J. Seixas de Melo, L. Macanita and F. Elisei, *J. Phys. Chem.* 1996, **100**, 18683. One of the reviewers suggested the charge transfer interactions between the [26]hexaphyrin networks and the oligothienyl substituents. But the solvent polarity effects were only marginal for **T1**-**T4** (SI).

11 (a) P. Morosini, M. Scherer, S. Meyer, V. Lynch and J. L. Sessler, *J. Org. Chem.* 1997, **62**, 8848; (b) J.-Y. Shin, S. S. Hepperle, B. O. Patrick and D. Dolphin, *Chem. Commun.* 2009, 2323; (c) S. Saito, K. Furukawa and A. Osuka, *J. Am. Chem. Soc.* 2010, **132**, 2128.

12 For the full Gaussian citation, see SI.

13 T. K. Ahn, J. H. Kwon, D. Y. Kim, D. W. Cho, D. H. Jeong, S. K. Kim, M. Suzuki, S. Shimizu, A. Osuka and D. Kim, *J. Am. Chem. Soc.* 2005, **127**, 12856.

14 Z. Chen, C. S. Wannere, C. Corminboeuf, R. Puchta and P. von R. Schleyer, *Chem. Rev.* 2005, **105**, 3842.

15 T. M. Krygowski and K. M. Cryański, *Chem. Rev.* 2001, **101**, 1385.